J Nanopart Res (2016)18:235
DOI 10.1007/s11051-016-3541-8

RESEARCH PAPER

Polyvinylpyrrolidone and arsenic-induced changes in biological responses of model aquatic organisms exposed to iron-based nanoparticles

Verónica Llaneza · Ismael Rodea-Palomares · Zuo Zhou · Roberto Rosal · Francisca Fernández-Pina · Jean-Claude J. Bonzongo

Received: 14 November 2015 / Accepted: 30 July 2016

Abstract The efficiency of zero-valent iron particles used in the remediation of contaminated groundwater has, with the emergence of nanotechnology, stimulated interest on the use of nano-size particles to take advantage of high-specific surface area and reactivity characteristics of nanoparticles (NPs). Accordingly, engineered iron-NPs are among the most widely used nanomaterials for in situ remediation. However, while several ecotoxicity studies have been conducted to investigate the adverse impacts of these NPs on aquatic organisms, research on the implications of spent iron-based NPs is lacking. In this study, a comparative approach is used, in which the biological effects of three iron-based NPs (Fe_3O_4 and γ-Fe_2O_3 NPs with particle sizes ranging from 20 to 50 nm, and Fe^0-NPs with an average particle size of 40 nm) on *Raphidocelis subcapitata* (formely known as *Pseudokirchneriella subcapitata*) and *Daphnia magna* were investigated using both as-prepared and pollutant-doped Fe-based NPs. For the latter, arsenic (As) was used as example sorbed pollutant. The results show that improved degree of NP dispersion by use of polyvinylpyrrolidone overlapped with both increased arsenic adsorption capacity and toxicity to the tested organisms. For *R. subcapitata,* Fe-oxide NPs were more toxic than Fe^0-NPs, due primarily to differences in the degree of NPs aggregation and ability to produce reactive oxygen species. For the invertebrate *D. magna*, a similar trend of biological responses was observed, except that sorption of As to Fe^0-NPs significantly increased the toxic response when compared to *R. subcapitata*. Overall, these findings point to the need for research on downstream implications of NP-pollutant complexes generated during water treatment by injection of NPs into aquatic systems.

Keywords Iron · Nanoparticles · Arsenic · Algae · Invertebrate · Toxicity · Environmental effects

Electronic supplementary material The online version of this article (doi:10.1007/s11051-016-3541-8) contains supplementary material, which is available to authorized users.

V. Llaneza · Z. Zhou · J.-C. J. Bonzongo (✉)
Engineering School of Sustainable Infrastructure and Environment, Department of Environmental Engineering Sciences, University of Florida,
PO Box 116450, Gainesville, FL 32611, USA
e-mail: bonzongo@ufl.edu

I. Rodea-Palomares · F. Fernández-Pina
Dept. de Biologia, Facultad de Ciencias, Univ. Autonoma de Madrid, 28049 Madrid, Spain

R. Rosal
Dept. de Ingeniería Química, Univ. de Alcalá, 28871 Alcalá de Henares, Madrid, Spain

Introduction

Engineered nanoparticles (NPs) are now produced and used worldwide and across an increasingly broad

Published online: 12 August 2016

range of applications. The apparent ubiquity of NPs increases their probability to come in contact with living organisms, therefore, raising concerns on the potential effects of these emerging pollutants. The anticipated adverse biological effects would likely occur at the *"NP-organism"* interfaces, with subsequent implications at both the organism and ecosystem levels (Nel and Xia 2006; Auffan et al. 2008; Kim et al. 2010a, b; Mostafa et al. 2011; Chen et al. 2011; Fang et al. 2011; Gao et al. 2011; Ma and Lin 2013).

Currently, metallic iron-based remediation technologies are taking advantage of the peculiar properties of NPs to remediate environmental compartments contaminated with organic (e.g., chlorinated organic solvents) and/or inorganic (e.g., arsenic, chromium and mercury) pollutants (Cornell 1996; Dixit and Hering 2003; Ponder et al. 2000; Cao and Zhang 2006; Sun et al. 2006; Li and Zhang 2006; Olegario et al. 2009; Vernon and Bonzongo 2014). In particular, nano-zero-valent iron particles, referred to later herein as Fe^0-NPs, have been suspended in aqueous slurries for injection in subsurface environments, in the direct vicinity of polluted sections of aquifers (Huang et al. 2008; Johnson et al. 2009). Fe^0-NPs have also been evaluated in wastewater treatment for nitrogen removal through chemical reduction of nitrate (Shin and Cha 2008; Hwang et al. 2012), as well as for phosphate removal through chemical precipitation (Shin and Cha 2008). For such applications, it has become a common practice to use stabilizing agents to obtain ideal NP suspensions and maximum sought effects (Pisanic 2007, Zhao et al. 2016). Example stabilizing agents commonly used to prepare iron-based NPs suspensions include polyethylene glycol (PEG) (Pisanic 2007, Gupta and Curtis 2004; Zhang et al. 2004), polyethyleneimine (PEI) (Chertok et al. 2010; Yang et al. 2011) in biomedical research, and polyvinylpyrrolidone (PVP) in environmental remediation studies (Saleh et al. 2008; Phenrat et al. 2006; Sakulchaicharoen et al. 2010). Besides the intentional introduction of NPs to the environment for remediation purposes, it is anticipated that the manufacturing, use, and disposal of NP-based products would likely result in environment pollution as well. Once introduced to natural systems, NPs could undergo transformations through both biotic and abiotic reactions. However, the impacts of such reactions on the bioavailability and potential toxicity of NPs remain largely unknown (Ma and Lin 2013). Accordingly, one potential issue related to the environmental application of nanotechnology which remains poorly addressed in current literature is the fate and the biological impacts of NP-pollutant complexes formed during remediation processes. In this study, a comparative approach is used to investigate the biological effects of three iron-based NPs (Fe_3O_4, γ-Fe_2O_3, and Fe^0) on a primary producer and a primary consumer. The primary producer used in the different dose-exposure experiments is *Raphidocelis subcapitata*, previously known as *Pseudokirchneriella subcapitata*, and will be referred to in this paper as *R. subcapitata*. *Daphnia magna* was used as example primary consumer. Tested NPs were used individually in bioassays as (i) water-suspended NPs, (ii) PVP-suspended NPs, and (iii) PVP-suspended NP-arsenic complexes.

Materials and methods

The following is a brief description of the different methods used in this study. A detailed description of used experimental methods and analytical techniques can be found in our earlier publication (Gonzalo et al. 2014).

Materials

Fe_3O_4 and γ-Fe_2O_3 NPs used in this study were purchased from Inframat® Advanced Materials LC (Connecticut, USA) with particle size ranging from 20 to 50 nm as reported by the manufacturer. The metallic iron (Fe^0) NPs used were purchased from Quantum-Sphere (California, USA), and had an average particle size of 40 nm. PVP was purchased from Sigma-Aldrich Chemical Co. (Missouri, USA). Arsenic pentoxide (As_2O_5) purchased from Alfa Aesar (Massachusetts, USA) was used to prepare solutions of different arsenate (AS^V) concentrations. The freshwater green algae, *R. subcapitata* was obtained from Microbiotests, Inc. (Denmark), while the freshwater invertebrate *D. magna* was purchased from "DAPHTOXKIT-FTM Magna" (Ghent, Belgium). All chemicals were reagent grade and used without further purification. NP suspensions were freshly prepared in

18.3 MΩ Milli-Q SP ultrapure water and characterized prior to use in all experiments.

Preparation and characterization of iron-based NP suspensions

Stock suspensions of Fe_3O_4, γ-Fe_2O_3, and Fe^0 NPs were prepared by suspending 50 mg of each of the three iron-based NPs in 50 mL of ultrapure water, followed by a 10 min ultrasonication using a Sonicator 3000 (Misonix, New York, USA). In addition to water-suspended NPs, Fe_3O_4, γ-Fe_2O_3, and Fe^0 NP suspensions were also prepared in a 5 wt% PVP aqueous solution and dispersed by ultrasonication as described above. The particle size distribution of the prepared NP suspensions and the ζ-potential of suspended NPs were determined using the Zetasizer Nano Instrument (Malvern Zetasizer). All measurements were carried out at 25 °C. About 1 mL of the sample suspension was transferred to a light-scattering cell and the temperature controlled within ±0.02°C. The analyses were started 10 min after the sample container was placed in the DLS instrument to allow the temperature to equilibrate. DLS measurements were conducted by performing 500 rounds of measurements in particle number mode. The ζ-potential was derived from electrophoretic mobility by applying the Henry equation and the Smoluchowski approximation (Gregory 2006). Finally, the specific surface area (SSA) was calculated from Eq. 1 (Macé et al. 2006), and where ρ is the density (g/cm^3) and d is the mean diameter (cm) of the suspended iron-based NP.

$$SSA = \frac{\pi \times d^2}{\rho \times \frac{\pi}{6} \times d^3}. \quad (1)$$

Arsenic sorption onto iron-based NPs suspended in either R. subcapitata or *D. magna*-specific growth media

Fe_3O_4, γ-Fe_2O_3, and Fe^0 NPs initially suspended in 5 wt% PVP aqueous solutions were added to growth media specific to *R. subcapitata* (Table SI-1) and *D. magna* (Table SI-2). The produced NP-containing growth media were then spiked with As, and then mixed continuously during the adsorption experiment using a roto-shaker®. The sorption capacity of each tested iron-based NP was determined in culture media without organisms by equilibrating As- and PVP-coated NP in a 0.01/1 ratio (*m/m*). This specific mass ratio was chosen based on preliminary tests conducted to ensure that >95 % of As initially present in solution was adsorbed onto NPs. Finally, after an equilibration time of 24 h, the prepared suspensions were centrifuged at 10,000 rpm and the supernatant removed and analyzed for both As and Fe concentrations by inductively coupled plasma mass spectrometry (ICP-MS).

Effect of iron-based NPs and arsenic on aquatic organisms

Pilot in situ studies of the remediation of contaminated groundwater reported in the literature use a broad range of nano-zero-valent iron concentrations, from values as low as 1.9 g/L (Zhang 2003), to up to 30 g/L as reported in a review by Mueller et al. (2012). For this laboratory study, the biological responses of the selected model organisms to NP-As complexes were investigated using dose-exposure experiments with As concentrations ranging from 10 µg/L (the minimum acceptable level for drinking water in the US) to 900 µg/L, and those of NPs ranging from 1 to 90 mg NP/L. These concentrations were selected based on the results of sorption and toxicity presented herein in Figs. 1 and 2. With regard to iron-based NPs, concentrations ranging from 1 to 90 mg NP/L were used to minimize (i) the interferences with algal growth resulting from dark slurry-like culture media and (ii) the concentration-dependent effect of Fe dissolution on optical density measurements (Gonzalo et al. 2014). The toxicity response was expressed as percent of either growth (*R. subcapitata*) or mobility (*D. magna*) inhibition. Experimental details for each of the two tested organisms are outlined below.

Growth inhibition experiments using *R. subcapitata*

The freshwater green algae *R. subcapitata* was grown using a method adapted from the US-EPA protocol (USEPA 2002) in 250 mL flasks (see Table SI-1 in the support information document) maintained at 28 °C under constant light conditions (ca. 65 µmol photons m^2s^{-1}) on a rotatory shaker setup at 120 rpm. For the different dose-exposure studies, only freshly prepared Fe_3O_4, γ-Fe_2O_3, and Fe^0 NP suspensions with and

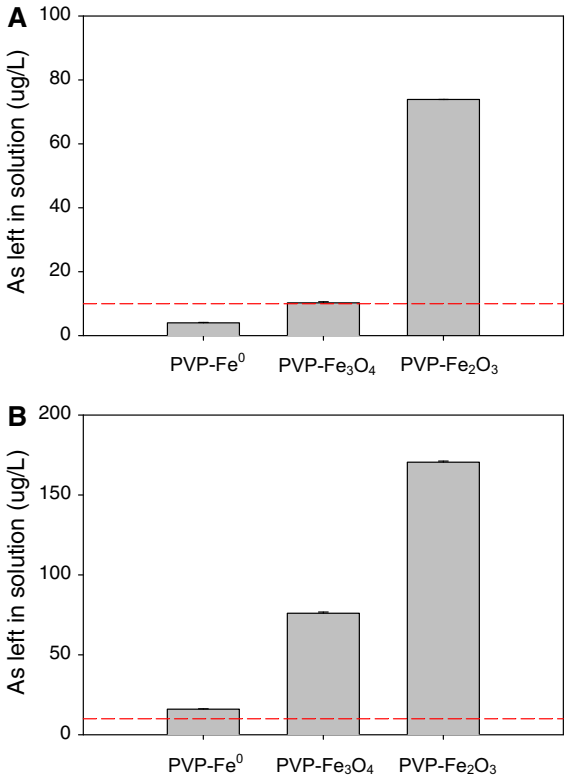

Fig. 1 Arsenic (As) removal efficiencies of PVP-coated Fe_3O_4, Fe_2O_3, and Fe^0 nanoparticles suspended individually in aqueous culture media used for growth of **a** the freshwater green algae, *R. subcapitata,* and **b** the freshwater invertebrate, *D. magna*. Arsenic concentrations were measured after a 24-h equilibration period ($n = 3$). The initial concentrations of each of the tested NPs and As in the culture media were 100 mg/L and 1000 µg/L, respectively. The horizontal dashed line corresponds to the US-EPA's action limit concentration of 10 µg As/L

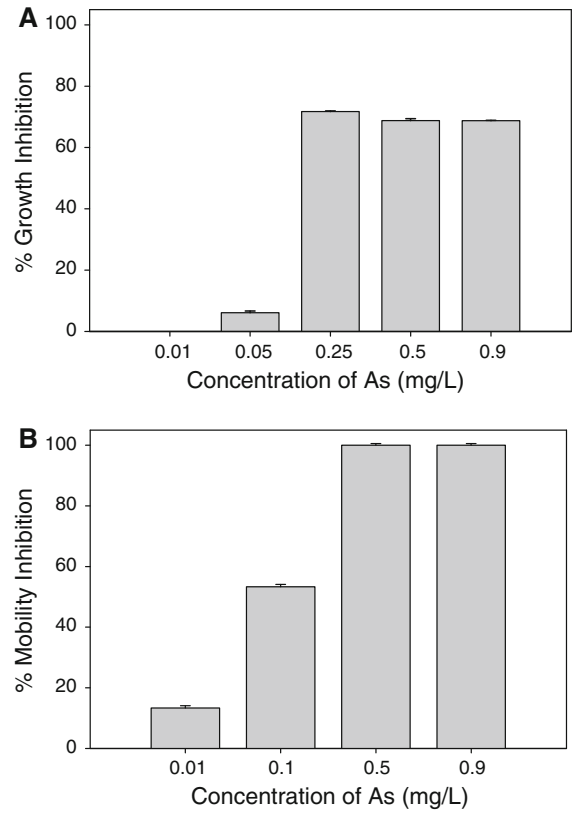

Fig. 2 Biological responses of *R. subcapitata* (**a**) and *D. magna* (**b**) grown in culture media containing As concentrations ranging from 0.01 to 0.9 mg/L. Results correspond to the average of triplicates for each tested concentration (*error bars* not visible when too small). Results are expressed as percent growth inhibition for the algae or percent mobility inhibition for the invertebrate

without PVP coating were used. As described above, the tested concentrations of NPs ranged from 0 (control sample) to 90 mg NP/L. Experiments exposing the test organisms to the iron-based NP suspensions were carried out in 6-well microplates placed on a GFL-3005 orbital shaker. Before exposure to the NPs, cultures were washed once and resuspended in the culture media to obtain a final optical density (OD) of 0.1 using a Hitachi U-2000 spectrophotometer and measuring absorbance at 750 nm ($OD_{750\ nm}$). Iron-based NPs were added to the culture-containing algal cells to achieve the desired NP concentrations. The dosed cultures were incubated for up to 72 h on a rotary shaker at 120 rpm and at 28 °C. For each treatment, experiments were performed in triplicates ($n = 3$), with serial dilutions as described in the standard OECD TG 201 method. Growth inhibition was used as endpoint for the algal-based toxicity assays, based on chlorophyll-a measurements. Bright-field micrographs were taken using an Olympus BH-2 microscope equipped with a Leica DC 300F digital camera to establish the presence or absence of physical NP-organism interactions.

Assessment of reactive oxygen species (ROS) generation

Reactive oxygen species (ROS) produced by *R. subcapitata* were assessed using the fluorescent dye 2′,7′-dichlorofluorescein diacetate (H_2DCFDA) obtained from Invitrogen Molecular Probes (Eugene, OR, USA). This technique is based on the fact that the intracellular oxidation of H_2DCFDA produces 2,7-

dichlorofluorescein (DCF), a fluorescent compound that serves as indicator of the presence of hydrogen peroxide and other ROS, such as hydroxyl and peroxyl radicals (Gonzalo et al. 2014). Briefly, A 10 mM H_2DCFDA stock solution was freshly prepared in DMSO under dim light conditions to avoid degradation. Prior to analysis, the algal cells were incubated for 30 min at room temperature in culture media containing a final H_2-DCFDA concentration of 10 μM. As a positive control for ROS formation, a 3 % H_2O_2 aqueous solution (v/v) was used. Fluorescence was monitored on a Synergy HT multimode microplate reader (BioTek, USA) with excitation and emission wavelengths of 488 and 530 nm, respectively. Results were normalized for differences in cell numbers, by measuring the chlorophyll content and expressed as arbitrary fluorescence units (AFU) per μg of chlorophyll-*(a + b)*.

Daphnia magna-based bioassays

Daphnia magna assays were based on the OECD standard procedure (OECD 2004). Briefly, hatching of the ephippia was initiated 3 days prior to the start of the acute toxicity tests in a synthetic growth media (Table SI-2 in support information document). Only young *D. magna* (age <24 h at the start of the test) were exposed to the different iron-based NP suspensions for a period of 48 h. At time 24 and 48 h after the beginning of the exposure period, individuals that were not able to swim after a sample agitation of 15 s were considered immobilized. Controls were not spiked with NPs, and all tests were conducted in triplicates. In addition to immobilization, any abnormal behavior or physical appearance such as organism external coating with particles or NP accumulation in the gut were noted. Bright-field micrographs were taken to confirm the presence, if any, of physical contact between NPs and organisms.

Results and discussion

Physical characteristics of iron-based nanoparticles used

Physical characteristics of NPs influence the extent of reactive site availability and have been linked to the biological responses of exposed organisms (Dabrunz et al. 2011). With regard to particle size, there is a general tendency of a severe adverse biological impact associated with organism's exposure to nano-size particles as compared to aggregated and large particles when studied under similar conditions (Dabrunz et al. 2011; Zhu et al. 2010). In this study, PVP was selected as stabilizing agent due to its reported nontoxic effect on several model aquatic organisms including those tested in this study (Oberdorster et al. 2007), as well as for its strong affinity for metals, which is driven primarily by the presence of pyrrolidone functional groups (Malynych et al. 2002).

Data on mean hydrodynamic diameter, ζ-potential, and SSA of both PVP-coated and water-suspended iron-based NPs are presented in Table 1. General trends of obtained results are as follows: NPs not stabilized by PVP show large hydrodynamic diameters, small SSA, and a net surface charge ranging from −24 to −30 mV. In contrast, PVP-coated NPs are characterized by much smaller hydrodynamic diameters and higher SSA, with a ζ-potential of about −18 mV due to charge masking by the coating polymer. In fact, PVP improves NP stability in aqueous suspensions through steric hindrance which occurs when PVP adsorbs onto the NPs (Sakulchaicharoen et al. 2010). The implication is minimization/prevention of particle–particle attraction, and therefore, limited particle aggregation (He and Zhao 2007; Sakulchaicharoen et al. 2010). In contrast, water-suspended iron-based NPs aggregated to form relatively large colloidal particles which precipitated out of solution rapidly.

Arsenic sorption onto iron-based nanoparticles suspended in *R. subcapitata* and *D. magna* growth media

Figure 1 shows the results of As removal onto PVP-coated Fe^0, Fe_3O_4, and γ-Fe_2O_3 NPs suspended in the two tested growth media. In the culture media used for the growth of *R. subcapitata*, As removal efficiency decreased in the following order: PVP-Fe^0 > PVP-Fe_3O_4 > PVP-Fe_2O_3 (Fig. 1a). However, under these specific experimental conditions, only PVP-Fe^0 and PVP-Fe_3O_4 NPs were able to decrease the dissolved As concentration from the initial level of 1000 μg/L (or 1 ppm) down to 4 and 10.25 μg/L, respectively. Comparatively, As sorption by PVP-Fe_2O_3 NPs was less efficient, with 73.87 μg/L left in solution after a

Table 1 Selected physical characteristics of Fe_3O_4, Fe_2O_3, and Fe^0 nanoparticles suspended in either plain water or in an aqueous solution of polyvinylpyrrolidone (PVP)

Nanoparticles (NPs)	Mean diameter (d) (nm)	Zeta potential (ζ) (mV)	Specific surface area (SSA) (m^2/g)
Fe_3O_4	370 ± 62.02	−30.19 ± 1.96	3.14
Fe_2O_3	256 ± 15.38	−24.69 ± 3.24	4.48
Fe^0	247 ± 94.73	−28.03 ± 1.77	3.63
PVP-Fe_3O_4	86 ± 6.58	−18.33 ± 1.24	13.56
PVP-Fe_2O_3	41 ± 10.68	−18.20 ± 1.03	28.27
PVP-Fe^0	28 ± 9.90	−18.40 ± 1.25	31.73

24-h equilibration period. On the other hand, while general trends of As sorption by NPs suspended in *D. magna*'s growth medium mimicked those obtained with the algal culture medium, As sorption efficiency dropped significantly (Fig. 1b). In fact, based on differences in the ionic strength, one would expect NPs in the algal culture medium (with higher concentrations of Ca^{2+} and Mg^{2+}) to undergo particle aggregation, and therefore, to result in a lower As sorption capacities as compared to the *D. magna*'s growth medium. Additionally for pH ranging between 7 and 8.5, typical of these growth media, the prevalent arsenic species should be $HAsO_4^{2-}$ under such oxygenated experimental conditions. Accordingly, it is likely that higher concentrations of Ca^{2+} and Mg^{2+} in the algal growth medium affect the net surface charge of NPs to favor sorption of the above As oxyanion species. Overall, these results point to the importance of solution chemistry specific to each growth medium on the ability of the tested iron-based NPs to sequester As from aqueous phase.

Figure 2 shows the responses of *R. subcapitata* (Fig. 2a) and *D. magna* (Fig. 2b) to increasing concentrations of As in growth media without NP addition. First, *R. subcapitata* exposed to As showed no toxic response in the culture medium containing As at a final concentration of 0.01 mg/L. However, a noticeable adverse biological response appears as the concentration of As reaches concentrations ≥0.25 mg/L, producing significant toxicity to algal cells, with a plateau-type response as As concentrations increased from 0.25 to 0.90 mg/L. Second, *D. magna*'s response to increasing As concentrations was different, in that, (i) organism immobilization was observed even in culture media with only 0.01 mg As/L, and (ii) the number of immobilized organisms exceeded 50 % when As concentration reached values ≥0.1 mg/L. Further increases in As concentration resulted in 100 % mobility inhibition (Fig. 2b).

Differences in the extent of biological responses expressed by *R. subcapitata* and *D. magna* could be dictated by several parameters including (i) the difference in the solution chemistry of each culture medium and its impact on As speciation and bioavailability, and (ii) differences in exposure pathways specific to each of these two model organisms. Algal cells can uptake As through protein channels earmarked for phosphorus, and once inside the cell, As can interfere with oxidative phosphorylation, interact with glucose and gluconate, and inhibit the activity of several enzymes (Hughes 2002). Unlike the tested green algae, the invertebrate *D. magna* is a particle feeder and is therefore exposed by a combination of ingestion of As adsorbed onto NPs and passive diffusion of dissolved As into cells. Previous studies have shown that as a chalcophile, arsenic can attach to sulfhydryl groups of molecules (Oremland and Stolz 2005) and result in toxicity (Sharma and Sohn 2009).

Biological responses of *R. subcapitata* to the iron-based NPs in the absence and presence of PVP and arsenic

Using iron-based NPs, three different sets of dose-exposure studies were conducted with *R. subcapitata* as the test organism and the obtained results are presented and discussed below.

First, using suspensions prepared in Nanopure® water, the biological impacts of Fe_3O_4, γ-Fe_2O_3, and Fe^0 NPs were investigated. The results are presented in Fig. 3. In this graph, the horizontal line corresponds to growth obtained from control culture media (i.e., no

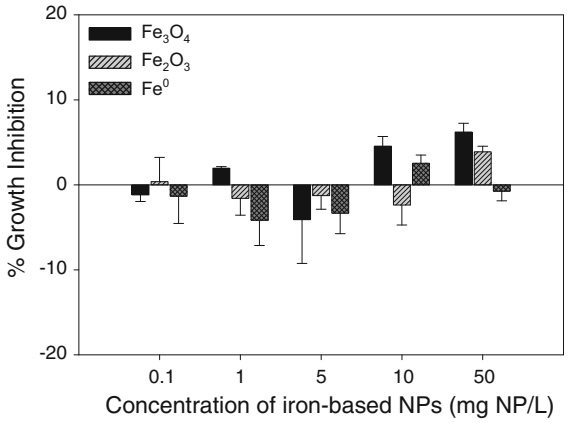

Fig. 3 Effects of increasing concentrations of water-suspended Fe_3O_4, Fe_2O_3, and Fe^0 NPs on the growth of *R. subcapitata*. Results are average of triplicate experiments and are expressed as percent growth inhibition using control media (no nanoparticles added) as reference corresponding to 0 % growth inhibition. *Negative values* indicate a tendency toward growth stimulation

NP added and no growth inhibition), which is used as reference. Accordingly, positive values correspond to growth inhibition while negative values point to growth stimulation. For the range of NP concentrations tested (0–50 mg/L), and taking into account the error bars on plotted data, it is obvious that these NPs have very little to no impact on *R. subcapitata* under these specific experimental conditions. In both cases (e.g., growth inhibition or stimulation), measured values were within 10 % of the reference or control values.

Based on data published in peer-reviewed literature, it is known that noncoated and water-suspended metallic Fe-NPs can adhere to cells and induce a reductive decomposition of functional groups in proteins, which in turn disrupts cell membrane functions due to the strong reductant character of iron ($EH°(Fe^{2+}/Fe^0) = -0.447$ V). In addition, since the change in redox potential is strongly dependent on the dose of metallic Fe-NPs in the culture media, direct interactions between NPs and cells should lead to an increasing trend of toxic response along the dose gradient. However, this is not the case in data obtained in this study. Trends of biological responses obtained here are likely dictated by a combination of factors including (i) the significance of physical contact between cells and NPs (Sadiq et al. 2011a, b), (ii) NPs agglomeration induced by algal-derived extracellular proteins rich in cysteine, those reported for bacteria cells (Moreau et al. 2007), and (iii) toxicity mitigation attributable to algal organic matter adsorbed onto NP surfaces through electro-steric hindrance (Chen et al. 2011; Lee et al. 2008). Overall, the result is a nonlinear dose–response relationship characterized by an irregular pattern as growth stimulation and inhibition alternate along the NP concentration gradients. Such nonlinear dose–response relationships, especially at low level exposures, are rather common and have been investigated in recent NP toxicity studies (Lavicoli et al. 2014; Gonzalo et al. 2014).

Second, the biological responses of *R. subcapitata* exposed to PVP-coated iron-based NPs were assessed in the absence and presence of As. The obtained

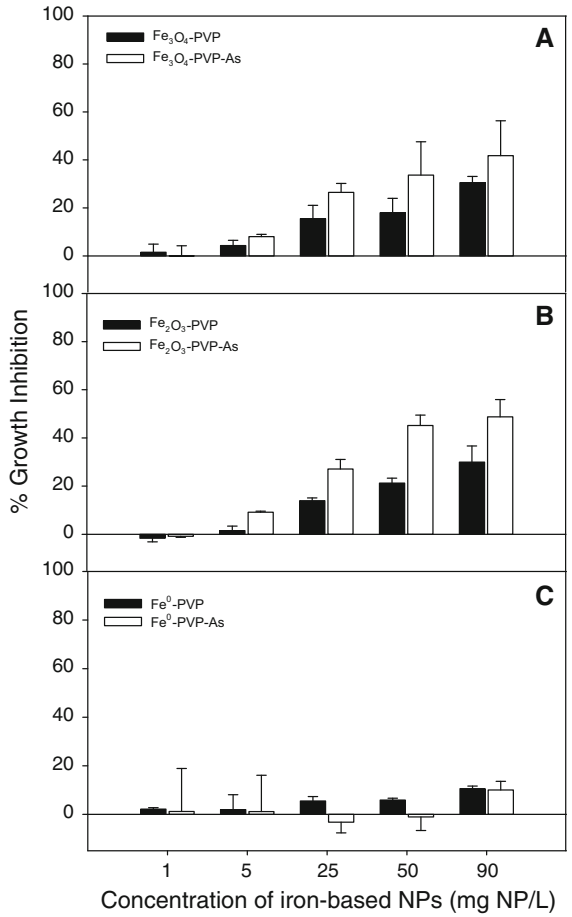

Fig. 4 Comparative study of the effects of polyvinylpyrrolidone (PVP)-coated iron-based NPs in the absence and presence of As on *R. subcapitata*: **a** PVP-coated Fe_3O_4, **b** PVP-coated Fe_2O_3, and **c** PVP-coated Fe^0

results are presented in Fig. 4. The recorded growth inhibition trends from these dose-exposure experiments are as follows: First, an increase in growth inhibition is observed with increasing NPs concentrations when algal cells are exposed to two of the PVP-coated iron oxide NPs (Fe_3O_4, γ-Fe_2O_3), and regardless of either the presence or absence of As adsorbed to the NPs (Fig. 4a, b). For the two tested PVP-coated Fe-oxide NPs, the presence of As resulted in increased toxicity, but differences were not always statistically different when compared to biological responses obtained in the absence of As. In contrast to the Fe-oxide NPs, PVP-coated Fe^0-NPs had a very limited adverse impact on exposed algal cells (Fig. 4c). Although the induced growth inhibition/stimulation were negligible (<10 %) along the tested Fe^0-NP concentration gradient, the use of PVP as stabilizing agent increased NP dispersion within the culture medium, resulting in a slight increase in growth inhibition trend. The presence of As produced a pattern which mimicked those reported earlier in Fig. 3, likely due to differences in NP net surface charges after sorption of As.

Overall, several parameters can be considered when explaining the above-described biological responses. Looking at the physical parameters, the use of PVP as a stabilizing agent improves NP dispersion and therefore the prevalence of nano-size particles in the suspension. This would limit the extent of particle aggregation in the culture medium, and therefore, increase the physical contact between NPs and algal cells over the short duration of bioassays conducted in this study. Microscopic observations of samples taken from these NP-treated algal cells showed the presence of heterogeneous aggregates made of algal cells and NPs (Figure SI-1 in support information document), suggesting that the recorded toxic responses were partly favored by direct physical contact between NPs and cells.

The above interpretation of the data holds true only for the two Fe-oxide NPs, but not for Fe^0-NPs. Results from previous research do suggest that the high toxicity of polymer-stabilized NPs is linked to the high reactivity of nano-size particles and their ability to produce reactive oxygen species (ROS) (Nel and Xia 2006; Dabrunz et al. 2011). Fe_3O_4 NPs have a higher ratio of $Fe^{(II)}/Fe^{(III)}$, higher redox reactivity, and dissolution rates than γ-Fe_2O_3-NPs, followed by Fe^0-NPs (Sidhu 1981; Gorski et al. 2009). Furthermore, Fe_3O_4 NPs are significantly more effective in producing hydroxyl radicals than γ-Fe_2O_3 NPs at the same nanoparticle total surface and reaction volume ratio (Voinov et al. 2010). Compared to Fe^0-NPs, the Fe-oxide NPs exhibit a higher catalytic efficiency in both hydrogen peroxide decomposition and hydroxyl radical production (Chen et al. 2012; Wu et al. 2014). Furthermore, at least one study investigated the reduction of metal oxide nanoparticles to zero valence forms, revealing that a zero-valent metal could potentially be bio-produced from corresponding metal oxide nanoparticles present in algal cultures (Gong et al. 2011). Therefore, soluble organic compounds produced by *R. subcapitata* may play a role in the reduction of Fe-oxide with adverse impact on algal growth.

Levels of oxidative stress within *R. subcapitata* growing in media containing iron-based NPs at a final concentration of 90 mg/L were measured as a function of time. The results are presented in Fig. 5. They show that the increase in oxidative stress corresponds to the increase in ROS production (data are normalized to the control data represented by the horizontal line set at 0 %). These results show an overall temporal increase in oxidative stress for the first 48 h in the Fe-oxide NP-treated culture media, followed by a decrease in measured % oxidative stress values (Fig. 5a, b). These results help explain the toxicity of Fe-oxide NPs to *R. subcapitata* presented earlier in Fig. 4a, b. ROS produced through chemical processes (Auffan et al. 2008; Pisanic 2007) would result in toxic effects, a well-studied and common paradigm involved in the adverse biological responses induced by several engineered NPs (Rodea-Palomares et al. 2012). Also, ROS injuries can induce the activation of apoptotic signaling pathways and ultimately cell death (Xiu et al. 2010). Our results on the production of ROS within algal membranes show that signs of oxidative stress are barely detectable in Fe^0-NP-treated algae (Fig. 5c), and no significant toxic response was expressed (Fig. 4c). These trends are likely due to the formation of large aggregates by Fe^0-NPs, a phenomenon which would negatively impact the previously reported formation of hydroxyl radicals by dissociative recombination of H_3O^+ catalyzed by the Fe^0/Fe^{II} redox couple (Zhaunerchyk et al. 2009; Kim et al. 2010a, b).

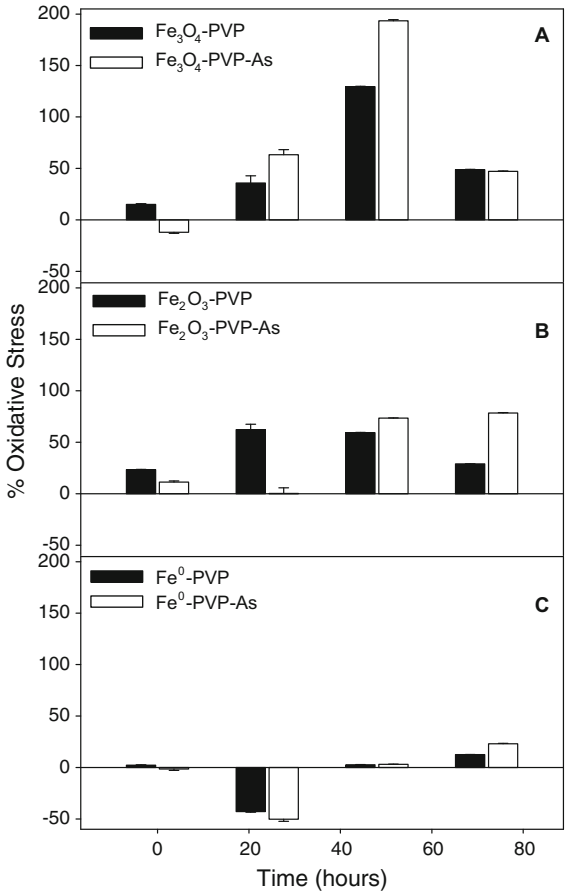

Fig. 5 Time-dependent induction of antioxidant and intracellular reactive oxygen species in *R. subcapitata* during exposure to polyvinylpyrrolidone (PVP)-coated iron-based NPs used at a final suspension concentration corresponding to 90 mg Fe/L. **a** PVP-coated Fe_3O_4, **b** PVP-coated Fe_2O_3, and **c** PVP-coated Fe^0

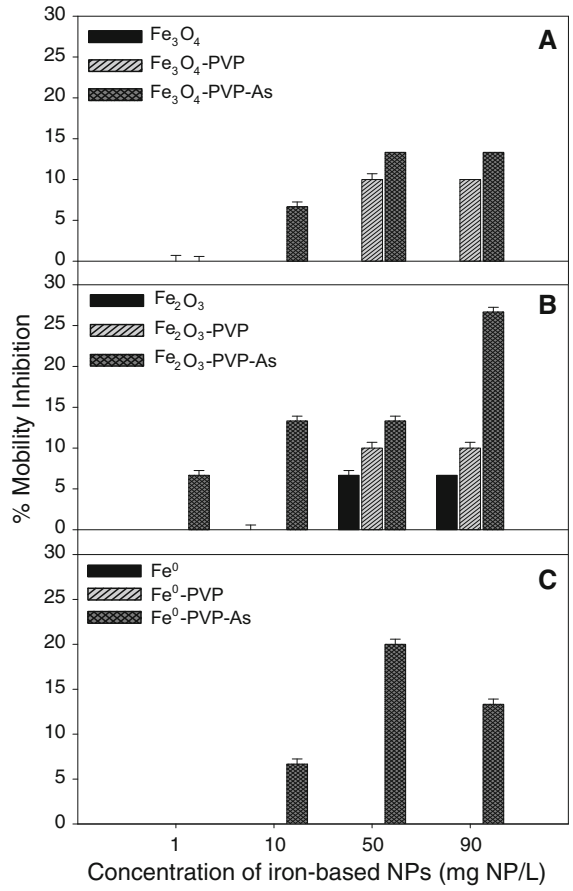

Fig. 6 Comparative study of the effects of polyvinylpyrrolidone (PVP)-coated iron-based NPs in the absence and presence of As on *D. magna*: **a** Fe_3O_4, **b** Fe_2O_3, and **c** Fe^0

Toxicity assay using the aquatic invertebrate *D. magna*

The results of *D. magna*-based toxicity bioassays are presented in Fig. 6. They show the biological responses in terms of percentage (%) of organisms immobilized as NP concentrations increased from 1 to 90 mg/L. For all tested iron-based NPs, the aqueous suspensions prepared without PVP had no toxicity effect on *D. magna*. This result is explained by lack of organism's exposure, which is limited under these specific experimental conditions by the removal from solution of aggregated NPs through sedimentation. This was obvious even by simple visual observations. In contrast, cultures treated with PVP-coated iron-based NPs induced mobility inhibition in all cases. Together, these results confirm that beside the chemical composition of NPs, the nano-size, reactivity, and dispersion stability of NPs are key parameters in the toxicity responses of exposed organisms (Dabrunz et al. 2011; Warheit et al. 2007).

As particle feeders, *D. magna* ingest particles, and previous studies have shown that food ingested by *D. magna* can have a residence time that ranges from about 3 to 60 min (Zhu et al. 2010). However, iron-based NPs ingested by *D magna* do not constitute a food source and their residence time could depend on a combination of factors including the size of ingested nanoparticles and rates of elimination. For instance, the accumulation of large aggregated NPs in the gut could affect elimination rates. In addition to NP ingestion by *D. magna*, Fe-based NPs have high binding affinity toward organic surfaces, resulting in a

steady growing layer of iron-oxide coating on exposed organisms through binding onto exoskeleton (Dabrunz et al. 2011). This is illustrated by the bright-field micrographs (Figure SI-2), and is a confirmation of direct contact NP organism. The formation of NP coatings onto *D. magna*'s exoskeleton could increase the weight of the organisms and result in physical resistance during swimming, hence, impacting mobility (Dabrunz et al. 2011).

In line with these studies, the acute test primarily on PVP-coated and water-suspended Fe_3O_4, γ-Fe_2O_3, and Fe^0 NPs with and without As adsorb onto NPs showed a significantly less toxicity compared to As alone in solution. Daily survival data indicated that the inhibition of the mobility of *D. magna* increased from 13.33 to 100 % when As concentration in solution increased from 0.01 to 0.5 mg/L. In fact, a micrograph of *D. magna* exposed to As alone without NPs (Figure SI-2B) shows the dramatic impact of As on this invertebrate. Finally, the presence of As made all tested NPs more toxic. Most important is the impact of As on Fe^0-NP toxicity. In the presence of As, metallic Fe-NPs displayed a highly significant toxicity effect as compared to the biological responses recorded from *D. magna* exposed to metallic Fe-NPs and no As. It appears that As enhances the toxicity of metallic Fe-NPs, and it is possible that a Trojan horse-like effect is responsible of the observed adverse biological effects.

Conclusion

This study focused on the potential toxicity of PVP-coated iron-based NPs and formed PVP-coated iron-based NP and arsenic complexes, which can form if iron-based NPs were to be used in water treatment processes. Based on the bioassays used in this study, the results suggest that the biological responses of exposed organisms would vary with both the chemical composition of NPs and types of aqueous suspensions (surfactant stabilized or not). Differences were obvious when comparing the biological impacts of Fe-oxide NPs to that of Fe^0-NPs, regardless of the tested model organisms. Overall, Fe-oxide NPs were more toxic than Fe^0-NPs, in either the presence or absence of arsenic adsorbed onto the NPs. However, it is important to note that the toxicological implications assessed in this study relied on short-term exposure experiments. While this approach takes into account the effect of water chemistry (e.g., pH, types of ions present, ionic strength, dissolved organic matter) on the recorded toxicity of tested NPs, it leaves out the potential role of NP aging and associated physico-chemical transformations that can be accounted for only through long-term exposure studies or by use of NPs aged in tested media. For instance, when Fe^0-NPs are injected into aquatic systems, they would certainly undergo corrosion which results in the formation of an encapsulating layer of surface oxide (Scott et al. 2010; Crane et al. 2011). In fact, the bulk of Fe^0-NPs injected into groundwater during a remediation process do form iron oxide particulates (Adeleye et al. 2013), and both the chemical composition and degree of crystallinity of such iron oxide minerals are not necessarily similar to Fe_3O_4 and γ-Fe_2O_3 tested in this study. On the other hand, over time, the buildup of exudates secreted by microorganisms could impact the stability of NPs, and therefore, their interactions with living organisms (Adeleye et al. 2016). Since toxicity results obtained from short-term exposure studies give a near-term insight into the potential biological impacts, further studies should emphasize long-term exposure experiments coupled with the characterization of the NPs as a function of time. Accordingly, whenever one looks at nZVI as treatment option for polluted water bodies, a long-term monitoring should be part of the strategy (Grieger et al. 2010).

Overall, findings from this study suggest that efforts to develop NP-based technologies for water treatment should take into account the fate of generated NP-toxicant wastes to avoid downstream negative impacts on ecosystem functions, and ultimately, human health.

Acknowledgments This research was supported by a seed grant from the University of Florida to JCB. VL was supported by the Bridge to the Doctorate Fellowship from the Office of Graduate Minority Programs in addition to a UF-Alumni Assistantship. We thank Joseph Marchionno from UF and Jennifer Quiros Jimenez of the Universidad de Alcalá for their help with different lab experiments and sample analysis. Finally, the authors thank the anonymous reviewers who helped improve the overall quality of the manuscript.

References

Adeleye AS, Keller AA, Miller RJ, Lenihan HS (2013) Persistence of commercial nano-scaled zero-valent iron (nZVI) and by-products. J Nanopart Res 15(1):1–18

Adeleye AS, Stevenson LM, Su Y, Nisbet RM, Zhang Y, Keller AA (2016) Influence of phytoplankton on fate and effects of modified zero-valent iron nanoparticles. Environ Sci Technol. doi:10.1021/acs.est.5b06251

Auffan MI, Achouak W, Rose JRM, Roncato M-A, Chaneac C, Waite DT, Masion A, Woicik JC, Wiesner MR, Bottero J-Y (2008) Relation between the redox state of iron-based nanoparticles and their cytotoxicity toward *Escherichia coli*. Environ Sci Technol 42(17):6730–6735

Cao J, Zhang W-X (2006) Stabilization of chromium ore processing residue (COPR) with nanoscale iron particles. J Hazard Mater 132(2–3):213–219

Chen J, Xiu Z, Lowry GV, Alvarez PJJ (2011) Effect of natural organic matter on toxicity and reactivity of nano-scale zero-valent iron. Water Res 45(5):1995–2001

Chen Z, Yin J-J, Zhou Y-T, Zhang Y, Song L, Song M, Hu S, Gu N (2012) Dual enzyme-like activities of iron oxide nanoparticles and their implication for diminishing cytotoxicity. ACS Nano 6(5):4001–4012

Chertok B, David AE, Yang VC (2010) Polyethyleneimine-modified iron oxide nanoparticles for brain tumor drug delivery using magnetic targeting and intra-carotid administration. Biomaterials 31(24):6317–6324

Cornell S (1996) The iron oxides; structure, properties, reactions, occurrence and uses, 1st edn. VCH, New York

Crane RA, Dickinson M, Popescu IC, Scott TB (2011) Magnetite and zero-valent iron nanoparticles for the remediation of uranium contaminated environmental water. Water Res 45:2931–2942

Dabrunz A, Duester L, Prasse C, Seitz F, Rosenfeldt R, Schilde C, Schaumann GE, Schulz R (2011) Biological surface coating and molting inhibition as mechanisms of tio_2 nanoparticle toxicity in *Daphnia magna*. PLOS One 6(5):e20112

Dixit S, Hering JG (2003) Comparison of As(V) and As(III) sorption onto iron oxide minerals: implications for arsenic mobility. Environ Sci Technol 37(18):4182–4189

Fang Z, Chen J, Qiu X, Qiu X, Cheng W, Zhu L (2011) Effective removal of antibiotic metronidazole from water by nanoscale zero-valent iron particles. Desalination 268(1–3): 60–67

Gao J, Wang Y, Hovsepyan A, Bonzongo J-C (2011) Effects of engineered nanomaterials on microbial catalyzed biogeochemical processes in sediments. J Hazard Mater 186(1):940–945

Gong N, Shao K, Feng W, Lin Z, Liang C, Sun Y (2011) Biotoxicity of nickel oxide nanoparticles and bio-remediation by microalgae *Chlorella vulgaris*. Chemosphere 83(4):510–516

Gonzalo S, Llaneza V, Pulido-Reyes G, Fernández-Piñas F, Bonzongo J-C, Leganes F, Rosal R, Garcia-Calvo E, Rodea-Palomares I (2014) A colloidal singularity reveals the crucial role of colloidal stability for nanomaterials in vitro toxicity testing: nZVI-microalgae colloidal system as a case study. PLOS One 9(10):e109645

Gorski CA, Nurmi JT, Tratnyek PG, Hofstetter TB, Scherer MM (2009) Redox behavior of magnetite: implications for contaminant reduction. Environ Sci Technol 44(1):55–60

Gregory J (2006) Particles in water properties and processes. Taylor & Francis, Boca Raton, p 180

Grieger KD, Fjordbøge A, Hartmann NB, Eriksson E, Bjerg PL, Baun A (2010) Environmental benefits and risks of zero-valent iron nanoparticles (nZVI) for in situ remediation: risk mitigation or trade-off? J Contam Hydrol 118(3–4):165–183

Gupta A, Curtis AG (2004) Surface modified superparamagnetic nanoparticles for drug delivery: interaction studies with human fibroblasts in culture. J Mater Sci Mater Med 15(4):493–496

He F, Zhao D (2007) Manipulating the size and dispersibility of zerovalent iron nanoparticles by use of carboxymethyl cellulose stabilizers. Environ Sci Technol 41(17):6216–6221

Huang Q, Shi X, Pinto RA, Petersen EJ, Weber WJ (2008) Tunable synthesis and immobilization of zero-valent iron nanoparticles for environmental applications. Environ Sci Technol 42(23):8884–8889

Hughes MF (2002) Arsenic toxicity and potential mechanisms of action. Toxicol Lett 133(1):1–16

Hwang Y, Kim D, Ahn Y-T, Moon C-M, Shin H-S (2012) Recovery of ammonium salt from nitrate-containing water by Iron nanoparticles and membrane contactor. Environ Eng Res 17:111–116

Johnson RL, Johnson GOB, Nurmi JT, Tratnyek PG (2009) Natural organic matter enhanced mobility of nano zerovalent iron. Environ Sci Technol 43(14):5455–5460

Kim H, Hong H-J, Jung J, Kim S-H, Yang J-W (2010a) Degradation of trichloroethylene (TCE) by nanoscale zero-valent iron (nZVI) immobilized in alginate bead. J Hazard Mater 176(1–3):1038–1043

Kim JY, Park HJ, Lee C, Nelson KL, Sedlak DL, Yoon J (2010b) Inactivation of *Escherichia coli* by nanoparticulate zerovalent iron and ferrous ion. Appl Environ Microbiol 76:7668–7670

Lavicoli I, Fontana L, Leso V, Calabrese EJ (2014) Hormetic dose-responses in nanotechnology studies. Sci Total Environ 487:361–374

Lee C, Kim JY, Lee WI, Nelson KL, Yoon J, Sedlak DL (2008) Bactericidal effect of zero-valent iron nanoparticles on *Escherichia coli*. Environ Sci Technol 42(13):4927–4933

Li X-Q, Zhang WX (2006) Iron nanoparticles: the core-shell structure and unique properties for Ni(II) sequestration. Langmuir 22(10):4638–4642

Ma S, Lin D (2013) The biophysicochemical interactions at the interfaces between nanoparticles and aquatic organisms: adsorption and internalization. Environ Sci Process Impact 15(1):145–160

Macé C, Desrocher S, Gheorghiu F, Kane A, Pupeza M, Cernik M, Kvapil P, Venkatakrishnan R, Zhang W-X (2006) Nanotechnology and groundwater remediation: a step forward in technology understanding. Remediat J 16(2):23–33

Malynych S, Luzinov I, Chumanov G (2002) Poly(Vinyl Pyridine) as a universal surface modifier for immobilization of nanoparticles. J Phys Chem B 106(6):1280–1285

Moreau JW, Weber PK, Martin MC, Gilbert B, Hutcheon ID, Banfield JF (2007) Extracellular proteins limit the dispersal of biogenic nanoparticles. Science 316(5831):1600–1603

Mostafa MG, Chen Y-H, Jean J-S, Liu C-C, Lee Y-C (2011) Kinetics and mechanism of arsenate removal by nanosized iron oxide-coated perlite. J Hazard Mater 187:89–95

Mueller NC, Braun J, Bruns J, Černík M, Rissing P, Rickerby D, Nowack B (2012) Application of nanoscale zero valent iron (nZVI) for groundwater remediation in Europe. Environ Sci Pollut Res 19(2):550–558

Nel A, Xia T, Mädler L, Li N (2006) Toxic potential of materials at the nano-level. Science 311(5761):622–627

Oberdorster G, Oberdorster E, Oberdorster J (2007) Concepts of nanoparticle dose metric and response metric. Environ Health Perspect 115(6):A290

OECD (2004) Test no. 202*: Daphnia sp.* acute immobilisation test. OECD Publishing, Paris

Olegario JT, Yee N, Miller M, Sczepaniak J, Manning B (2009) Reduction of Se(VI) to Se(-II) by zerovalent iron nanoparticle suspensions. J Nanopart Res 12(6):2057–2068

Oremland RS, Stolz JF (2005) Arsenic, microbes and contaminated aquifers. Trends Microbiol 13(2):45–49

Phenrat T, Saleh N, Sirk K, Tilton RD, Lowry GV (2006) Aggregation and sedimentation of aqueous nanoscale zerovalent iron dispersions. Environ Sci Technol 41(1): 284–290

Pisanic tr, Blackwell JD, Shubayev VI, Finones RR, Jin S (2007) Nanotoxicity of iron oxide nanoparticle internalization in growing neurons. Biomaterials 28(16):2572–2581

Ponder SM, Darab JG, Mallouk TE (2000) Remediation of Cr(VI) and Pb(II) aqueous solutions using supported, nanoscale zero-valent iron. Environ Sci Technol 34(12): 2564–2569

Rodea-Palomares I, Gonzalo S, Santiago-Morales J, Leganés F, García-Calvo E, Rosal R, Fernández-Piñas F (2012) An insight into the mechanisms of nanoceria toxicity in aquatic photosynthetic organisms. Aquat Toxicol 122–123:133–143

Sadiq IM, Dalai S, Chandrasekaran N, Mukherjee A (2011a) Ecotoxicity study of titania (TiO_2) NPs on two microalgae species: *Scenedesmus sp*. and *Chlorella sp*. Ecotoxicol Environ Saf 74(5):1180–1187

Sadiq IM, Pakrashi S, Chandrasekaran N, Mukherjee A (2011b) Studies on toxicity of aluminum oxide (Al_2O_3) nanoparticles to microalgae species: *Scenedesmus sp*. and *Chlorella sp*. J Nanopart Res 13(8):3287–3299

Sakulchaicharoen N, O'Carroll DM, Herrera JE (2010) Enhanced stability and de-chlorination activity of pre-synthesis stabilized nanoscale FePd particles. J Contam Hydrol 118(3–4):117–127

Saleh N, Kim H-J, Phenrat T, Matyjaszewski K, Tilton RD, Lowry GV (2008) Ionic strength and composition affect the mobility of surface-modified fe0 nanoparticles in water-saturated sand columns. Environ Sci Technol 42(9):3349–3355

Scott TB, Dickinson M, Crane RA, Riba O, Hughes GM, Allen GC (2010) The effects of vacuum annealing on the structure and surface chemistry of iron nanoparticles. J Nanopart Res 12:1765–1775

Sharma VK, Sohn M (2009) Aquatic arsenic: toxicity, speciation, transformations, and remediation. Environ Int 35(4): 743–759

Shin K-H, Cha DK (2008) Microbial reduction of nitrate in the presence of nanoscale zero-valent iron. Chemosphere 72(2):257–262

Sidhu PS (1981) Dissolution of iron oxides and oxyhydroxides in hydrochloric and perchloric acids. Clay Clay Miner 29(4):269–276

Sun Y-P, Li X-Q, Cao J, Zhang W-X, Wang HP (2006) Characterization of zero-valent iron nanoparticles. Adv Colloid Interface Sci 120(1–3):47–56

US-EPA (2002) Test method 1003.0—Green algae, *Selenastrum capriconutum*, Growth

Vernon JD, Bonzongo J-CJ (2014) Volatilization and sorption of dissolved mercury by metallic iron of different particle sizes: implications for treatment of mercury contaminated water effluents. J Hazard Mater 276:408–414

Voinov MA, Pagan JOS, Morrison E, Smirnova TI, Smirnov AI (2010) Surface-mediated production of hydroxyl radicals as a mechanism of iron oxide nanoparticle biotoxicity. J Am Chem Soc 133(1):35–41

Warheit DB, Hoke RA, Finlay C, Donner EM, Reed KL, Sayes CM (2007) Development of a base set of toxicity tests using ultrafine TiO_2 particles as a component of nanoparticle risk management. Toxicol Lett 171(3):99–110

Wu H, Yin J-J, Wamer WG, Zeng M, Lo YM (2014) Reactive oxygen species-related activities of nano-iron metal and nano-iron oxides. J Food Drug Anal 22(1):86–94

Xiu Z-M, Gregory KB, Lowry GV, Alvarez PJJ (2010) Effect of bare and coated nanoscale zerovalent iron on tceA and vcrA gene expression in *Dehalococcoides spp*. Environ Sci Technol 44(19):7647–7651

Yang X, Hong H, Grailer JJ, Rowland IJ, Javadi A, Hurley SA, Xiao Y, Yang Y, Zhang Y, Nickles RJ, Cai W, Steeber DA, Gong S (2011) cRGD-functionalized, DOX-conjugated, and 64Cu-labeled superparamagnetic iron oxide nanoparticles for targeted anticancer drug delivery and PET/MR imaging. Biomaterials 32(17):4151–4160

Zhang W-X (2003) Nanoscale iron particles for environmental remediation: an overview. J Nanopart Res 5(3):323–332

Zhang Y, Sun C, Kohler N, Zhang M (2004) Self-assembled coatings on individual monodisperse magnetite nanoparticles for efficient intracellular uptake. Biomed Microdevice 6(1):33–40

Zhao X, Liu W, Cai Z, Han B, Qian T, Zhao D (2016) An overview of preparation and applications of stabilized zero-valent iron nanoparticles for soil and groundwater remediation. Water res 100:245–266

Zhaunerchyk V, Geppert WD, Rosen S, Vigren E, Hamberg M, Kamińska M, Kashperka I, af Ugglas M, Semaniak J, Larsson M, Thomas RD (2009) Investigation into the vibrational yield of OH products in the OH^+ H^+ H channel arising from the dissociative recombination of H_3O^+. J Chem Phys 130:214302

Zhu X, Chang Y, Chen Y (2010) Toxicity and bioaccumulation of TiO_2 nanoparticle aggregates in *Daphnia magna*. Chemosphere 78(3):209–215